

Remotely sensed transport in microwave photoexcited GaAs/AlGaAs two-dimensional electron system

Tianyu Ye,¹ R. G. Mani,¹ and W. Wegscheider²

¹*Department of Physics and Astronomy, Georgia State University, Atlanta, Georgia 30303, USA*

²*Laboratorium für Festkörperphysik, ETH Zürich, 8093 Zürich, Switzerland*

(Dated: 15 February 2018)

We demonstrate a strong correlation between the magnetoresistive and the concurrent microwave reflection from the microwave photo-excited GaAs/AlGaAs two-dimensional electron system (2DES). These correlations are followed as a function of the microwave power, the microwave frequency, and the applied current. Notably, the character of the reflection signal remains unchanged even when the current is switched off in the GaAs/AlGaAs Hall bar specimen. The results suggest a perceptible microwave-induced change in the electronic properties of the 2DES, even in the absence of an applied current.

Microwave semiconductor devices have had a profound impact on the fields of satellite and ground based communications, radar, and missile guidance,¹ and related technological developments have fueled motivation for additional basic research on semiconductors such as, for example, the GaAs/AlGaAs two-dimensional electron system. Meanwhile, the ever-improving electron mobility in the high mobility GaAs/AlGaAs 2DES continues to reveal electronic effects induced by microwave and terahertz photo-excitation, such as, for example, the zero-resistance state, without concurrent Hall resistance quantization,^{2,3} observed in the GaAs/AlGaAs 2DES, when the specimen is subjected to microwave and terahertz photo-excitation in a magnetic field. The experimental realization of such radiation-induced zero-resistance states, and associated B^{-1} -periodic radiation-induced magnetoresistance oscillations expanded the experimental²⁻²⁰ and theoretical²¹⁻³⁹ investigations of transport in the photo-excited 2-dimensional electron system.

Various mechanisms exist for understanding the radiation-induced magnetoresistance oscillations including radiation-assisted indirect inter-Landau-level scattering by phonons and impurities (the displacement model),^{21,23,25,31} non-parabolicity effects in an ac-driven system (the non-parabolicity model),²⁴ a radiation-induced steady state non-equilibrium distribution (the inelastic model),²⁶ and the periodic motion of the electron orbit centers under irradiation (the radiation driven electron orbit model).²⁸ According to theory, the experimentally observed zero-resistance states result from either a current instability^{22,30} or from the accumulation/depletion of carriers at the contacts.³⁶

Here, we compare the oscillatory magnetoresistive response of the microwave photo-excited GaAs/AlGaAs 2D electron system with the concurrent microwave reflection that is detected by a nearby resistance sensor. We report strong correlations, which are followed as a function of the microwave power, the microwave frequency, and the applied current. Notably, the character of the reflection signal remains unchanged even when the current is switched off in the GaAs/AlGaAs Hall bar specimen. The results suggest a perceptible microwave-induced change in the electronic properties of the 2DES, even in the absence of an applied current.

GaAs/AlGaAs Hall bars were mounted at the end of a long cylindrical waveguide along with a carbon resistor to sense the microwave reflection as shown in Fig. 1. The carbon sensor exhibits a strong negative temperature coefficient, i.e., $dR_s/dT \leq 0$. Thus, sensor heating by microwaves reflected from the 2DES produces a reduction in the sensor resistance

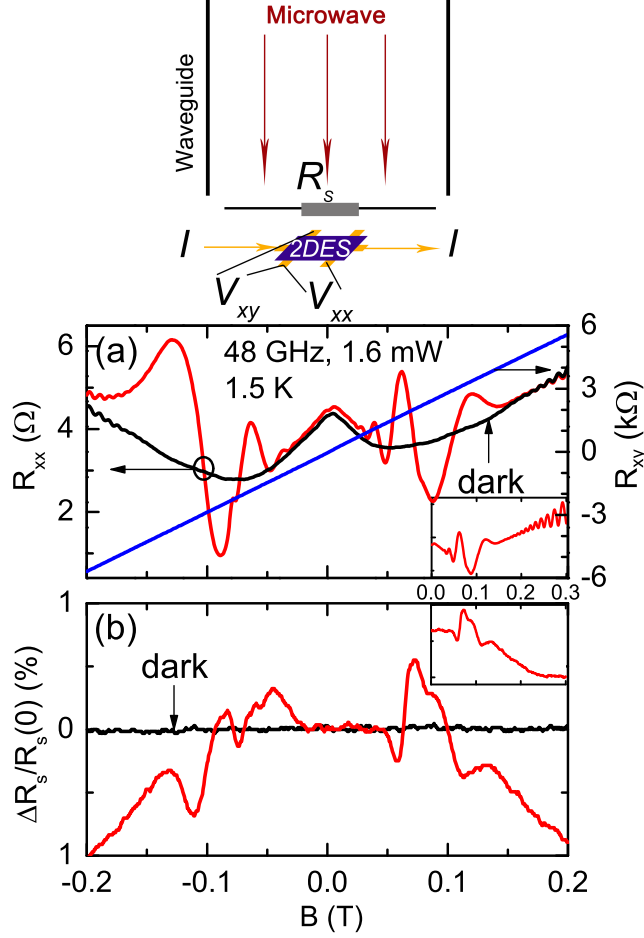


FIG. 1. (Color online) Top: A schematic of the measurement configuration showing the GaAs/AlGaAs Hall bar and the remote sensing resistor, R_s , located at the bottom of a cylindrical waveguide, within a low temperature cryostat. The panels (a) and (b) show the diagonal resistance (R_{xx}), Hall resistance (R_{xy}) and the fractional change of the remote detector resistance ($\Delta R_s/R_s(0)$) as functions of magnetic field, B , of sample S1. (a) R_{xx} (left panel) and R_{xy} (right panel) of S1 with (red curve) and without (black curve) 48 GHz microwave illumination. (b) Concurrent measurement of $\Delta R_s/R_s(0)$ with (red curve) and without (black curve) 48 GHz microwave excitation. The insets of (a) and (b) show the photoexcited R_{xx} and $\Delta R_s/R_s(0)$ signals over a broader B -range.

R_s , which becomes the signature of microwave reflection (or emission). The waveguide sample holder was inserted into a variable temperature insert in a superconducting solenoid. A base temperature of approximately 1.5 K was realized by pumping on the liquid helium within the variable temperature insert. The 2D electron density $n \approx 2.3 \times 10^{11} \text{ cm}^{-2}$ and

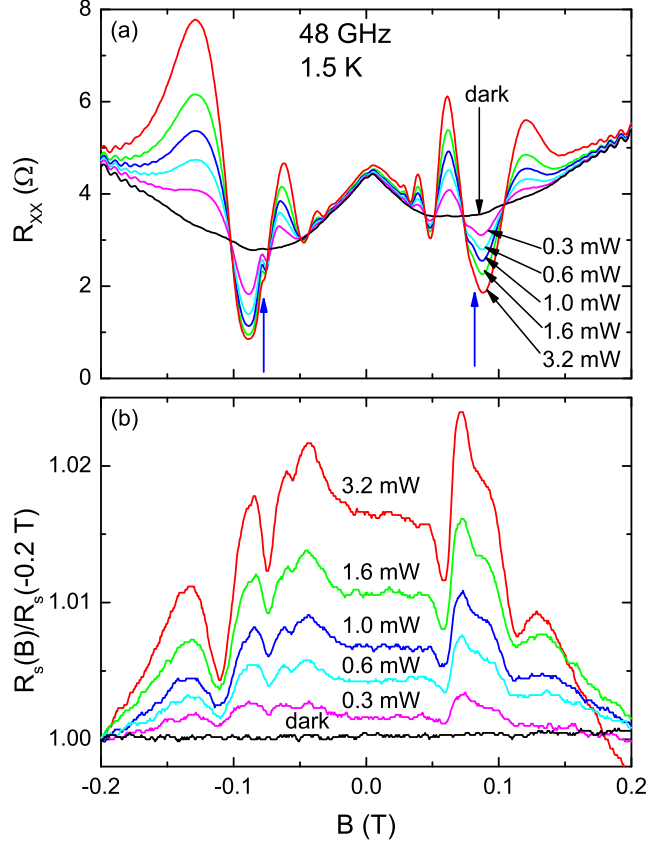


FIG. 2. (Color online) (a) The dark- and photoexcited- at 48 GHz R_{xx} signal, and (b) the concurrently measured normalized remotely sensed signal $R_s/R_s(-0.2 \text{ T})$ for a high mobility GaAs/AlGaAs specimen. Various colored traces correspond to the different power levels over the range $0 \leq p \leq 3.2 \text{ mW}$. The blue upward arrows in (a) point out the inflections on the oscillatory resistance.

the mobility $\mu \approx 8 \times 10^6 \text{ cm}^2/\text{Vs}$. Thus, the transport lifetime is $\tau \approx 3 \times 10^{-10} \text{ s}$ and the single particle lifetime $\tau_s \approx 2.8 \times 10^{-12} \text{ s}$. Finally, a low frequency lock-in technique was adopted to detect the electrical signals of interest.

Figure 1 compares the diagonal resistance R_{xx} (Fig. 1(a)) of a high mobility GaAs/AlGaAs sample and the concurrently measured remote detector resistance R_s (Fig. 1(b)). Fig. 1(a) shows that the sample in the dark, i.e., without microwave photo-excitation, does not exhibit microwave-radiation-induced magneto-resistance oscillations in R_{xx} , as the fractional change in the reflection detector signal $\Delta R_s/R_s$, see Fig. 1(b), is featureless as well in the dark. However, with 48 GHz microwave photoexcitation, see Fig. 1(a) and Fig. 1(b), R_{xx} exhibits microwave induced magnetoresistance oscillations for $-0.2 \leq B \leq 0.2 \text{ Tesla}$, see the

red trace in Fig. 1(a), and $\Delta R_s/R_s$ conveys an oscillatory reflection. Here, the microwave-induced changes in the detector signal $\Delta R_s/R_s(0) \approx 1\%$, where $\Delta R_s = R_s(B) - R_s(0)$, $R_s(B)$ is the sensor resistance in the magnetic field, and $R_s(0)$ is the zero-field sensor resistance. To confirm that the microwave induced effect in $\Delta R_s/R_s$ is due to the microwave response of the high-mobility GaAs/AlGaAs specimen, we have also examined low mobility GaAs/AlGaAs specimens in the same experimental setup. The results showed little difference between the photo-excited- and dark- R_{xx} , and also $\Delta R_s/R_s$ in the low mobility specimen, which is attributed to the absence of radiation-induced oscillations in the low mobility specimen. Finally, the insets of Fig. 1 (a) and (b) show that where R_{xx} in the high mobility specimen exhibits only Shubnikov-de Haas oscillations, R_s monotonically decreases as B is increased, but oscillatory features are not observable.

Figure 2 exhibits the microwave power (P)-dependence of R_{xx} - and the normalized R_s -, i.e., $R_s/R_s(-0.2 \text{ T})$, vs. B . The exhibited traces indicate the following features with changing microwave power: i) The phase of the microwave radiation-induced magnetoresistance oscillations in R_{xx} does not change with the microwave power, but oscillation amplitude increases with the power, P , over the range $0.3 \leq P \leq 3.2 \text{ mW}$. ii) Correspondingly, the oscillatory reflection conveyed by $R_s/R_s(-0.2 \text{ T})$ remains in phase for different microwave powers, although the relative amplitude increases with P . Note that the reflection response in Fig. 2 is not just confined to the vicinity of cyclotron resonance ($B \approx 0.11 \text{ Tesla}$).

Figure 3 examines the current (I) dependence of $V_{xx} = IR_{xx}$ and R_s at 35 GHz and $P = 3.2 \text{ mW}$. Here V_{xx} has been plotted rather than R_{xx} because R_{xx} is undefined when $I = 0 \mu\text{A}$. As the applied current, I , is decreased from $2.5 \mu\text{A}$ to $0 \mu\text{A}$, the diagonal voltage V_{xx} decreases proportionally, see Fig. 3(a), as expected. Fig. 3(b) exhibits the concurrently measured remotely sensed signal R_s at the same currents, I . Here, note the insensitivity in the R_s signal to the applied current.

To convey the remarkable feature in this result, in Fig. 4, we exhibit the V_{xx} vs. B and R_s vs. B now with 48 GHz microwave excitation at 3.2 mW, with the applied current $I = 1 \mu\text{A}$, in Fig. 4(a) and Fig. 4(b), and $I = 0 \mu\text{A}$ in Fig. 4(c) and Fig. 4(d). When the applied current is switched off, the V_{xx} signal vanishes as illustrated in Fig. 4(c). However, the non-monotonic variation in R_s due to the microwave reflection from the photoexcited 2DES persists even in the absence of the applied current. These features indicate that there is a microwave-induced response in the 2DES even in the absence of an applied current.

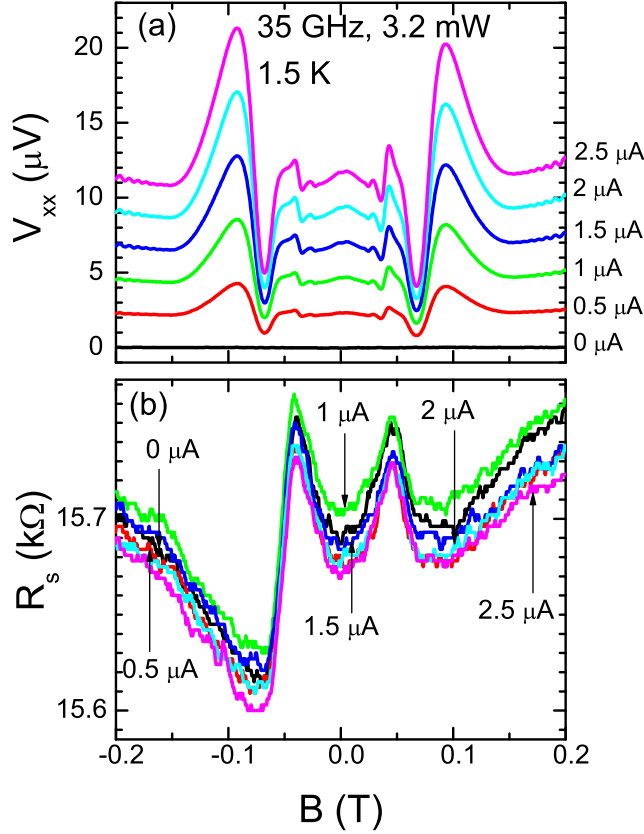


FIG. 3. (Color online) The diagonal voltage V_{xx} and the remote sensor resistance R_s are exhibited for a GaAs/AlGaAs specimen S1 under 35 GHz microwave excitation. The different color curves correspond to discrete applied currents, I , through sample with $0 \leq I \leq 2.5 \mu\text{A}$. The same color code has been used in the top and bottom panels.

We provide a brief explanation of the observed features using the theory of Lei and Liu.^{25,27} They asserted that, in the presence of impurity and phonon scattering, which couple the c.m. and relative motions, the microwave field affects the relative motion by allowing transitions between different states, leading to radiation-induced magnetoresistance oscillations.²⁵ Their calculations indicated oscillations in the energy absorption rate, S_p , which correlated with resonant oscillations in the electron temperature.²⁷ Although the theory did not explicitly examine the S_p in the limit of a vanishing applied electric field or current, it appears plausible that the energy absorption rate of the 2DES might be independent of whether or not an applied electric field or current exists in the specimen. If the S_p continued to exhibit resonant oscillations even without an applied current or electric field, then it seems plausible that the reflected microwave power would follow the oscillatory S_p .

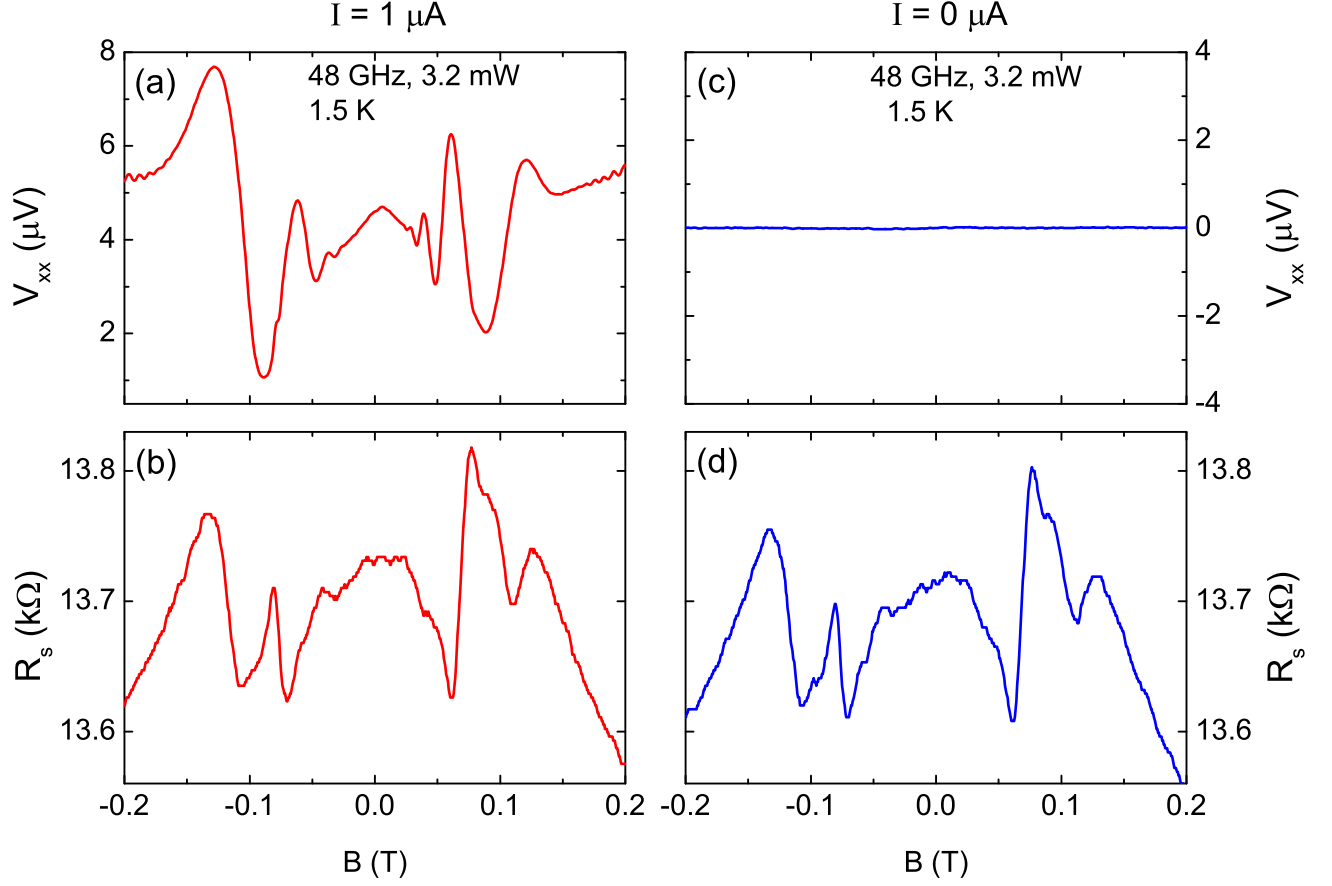


FIG. 4. (Color online) The diagonal voltage V_{xx} and the remotely sensed signal R_s for a GaAs/AlGaAs 2DES subjected to 48 GHz microwave excitation. In plots (a) and (b), the applied current $I = 1 \mu\text{A}$. Plots (c) and (d) correspond to $I = 0 \mu\text{A}$. Note that the R_s signal remains unchanged upon switching off the current through the specimen.

and also exhibit oscillations as seen in the experimental data here. Therefore, one might tentatively attribute the oscillations in the remotely sensed signal R_s to the oscillatory variation in the energy absorption rate of the microwave photo-excited 2DES and the concomitant change in the reflection.

In the radiation driven electron orbit model,²⁸ one expects a periodic back- and forth- radiation driven motion of the electron orbits. Since such oscillatory motion of electron charge is, from the classical perspective, expected to produce radiation, such reflection/emission signal reported by R_s might be expected. A full theory of this has not yet been published.

In summary, the magnetoresistive response of the microwave photo-excited GaAs/AlGaAs 2D electron system has been compared with the concurrent microwave reflection from the

2DES. The experimental results indicate a strong correlation between the observed features in the two types of measurements. Curiously, the character of the reflection signal remains unchanged even when the current is switched off in the GaAs/AlGaAs Hall bar specimen. The results suggest that the 2DES is microwave active even in the absence of an applied current.

Basic research at Georgia State University (GSU) is supported by the DOE-BES, MSE Division under de-sc0001762. Additional support for microwave work is provided by the ARO under W911NF-07-01-0158.

REFERENCES

- ¹J-F. Luy, *Microwave Semiconductor Devices: Theory, Technology, and Performance*, (Expert-Verlag, Renningen, 2005).
- ²R. G. Mani, J. H. Smet, K. von Klitzing, V. Narayanamurti, W. B. Johnson, and V. Umansky, *Nature* **420**, 646 (2002).
- ³M. A. Zudov, R. R. Du, L. N. Pfeiffer, and K. W. West, *Phys. Rev. Lett.* **90**, 046807 (2003).
- ⁴R. G. Mani, V. Narayanamurti, K. von Klitzing, J. H. Smet, W. B. Johnson, and V. Umansky, *Phys. Rev. B* **70**, 155310 (2004); *Phys. Rev. B* **69**, 161306 (2004).
- ⁵R. G. Mani, J. H. Smet, K. von Klitzing, V. Narayanamurti, W. B. Johnson, and V. Umansky, *Phys. Rev. Lett.* **92**, 146801 (2004); *Phys. Rev. B* **69**, 193304 (2004).
- ⁶R. G. Mani, *Physica E* **22**, 1 (2004); *Physica E*. **25**, 189 (2004).
- ⁷A. E. Kovalev, S. A. Zvyagin, C. R. Bowers, J. L. Reno, and J. A. Simmons, *Solid State Commun.* **130**, 379 (2004).
- ⁸B. Simović, C. Ellenberger, K. Ensslin, H. P. Tranitz, and W. Wegscheider, *Phys. Rev. B* **71**, 233303 (2005).
- ⁹S. A. Studenikin, M. Potemski, A. Sachrajda, M. Hilke, L. N. Pfeiffer, and K. W. West, *Phys. Rev. B* **71**, 245313 (2005).
- ¹⁰R. G. Mani, *Phys. Rev. B* **72**, 075327 (2005); *Appl. Phys. Lett.* **91**, 132103 (2007); *Appl. Phys. Lett.* **92**, 102107 (2008); *Physica E* **40**, 1178 (2008).
- ¹¹J. H. Smet, B. Gorshunov, C. Jiang, L. Pfeiffer, K. West, V. Umansky, M. Dressel, R. Meisels, F. Kuchar, and K. von Klitzing, *Phys. Rev. Lett.* **95**, 116804 (2005).

- ¹²A. Wirthmann, B. D. McCombe, D. Heitmann, S. Holland, K. Friedland, and C. M. Hu, Phys. Rev. B **76**, 195315 (2007).
- ¹³S. Wiedmann, G. M. Gusev, O. E. Raichev, T. E. Lamas, A. K. Bakarov, and J. C. Portal, Phys. Rev. B **78**, 121301 (2008).
- ¹⁴D. Konstantinov and K. Kono, Phys. Rev. Lett. **103**, 266808 (2009).
- ¹⁵R. G. Mani, W. B. Johnson, V. Umansky, V. Narayanamurti, and K. Ploog, Phys. Rev. B **79**, 205320 (2009).
- ¹⁶R. G. Mani, C. Gerl, S. Schmult, W. Wegscheider, and V. Umansky, Phys. Rev. B **81**, 125320 (2010).
- ¹⁷O. M. Fedorych, M. Potemski, S. A. Studenikin, J. A. Gupta, Z. R. Wasilewski, and I. A. Dmitriev, Phys. Rev. B **81**, 201302 (2010).
- ¹⁸A. N. Ramanayaka, R. G. Mani, and W. Wegscheider, Phys. Rev. B **83**, 165303 (2011).
- ¹⁹R. G. Mani, A. N. Ramanayaka, W. Wegscheider, Phys. Rev. B **84**, 085308 (2011); A. N. Ramanayaka, R. G. Mani, J. Iñarrea, and W. Wegscheider, Phys. Rev. B **85**, 205315 (2012)..
- ²⁰R. G. Mani, J. Hankinson, C. Berger, and W. A. de Heer, Nat. Commun. **3**, 996 (2012).
- ²¹A. C. Durst, S. Sachdev, N. Read, and S. M. Girvin, Phys. Rev. Lett. **91**, 086803 (2003).
- ²²A. V. Andreev, I. L. Aleiner, and A. J. Millis, Phys. Rev. Lett. **91**, 056803 (2003).
- ²³V. Ryzhii and R. Suris, J. Phys. Condens. Matter **15**, 6855 (2003).
- ²⁴A. A. Koulakov and M. E. Raikh, Phys. Rev. B **68**, 115324 (2003).
- ²⁵X. L. Lei and S. Y. Liu, Phys. Rev. Lett. **91**, 226805 (2003).
- ²⁶I. A. Dmitriev, M. G. Vavilov, I. L. Aleiner, A. D. Mirlin, and D. G. Polyakov, Phys. Rev. B **71**, 115316 (2005).
- ²⁷X. L. Lei and S. Y. Liu, Phys. Rev. B **72**, 075345 (2005).
- ²⁸J. Iñarrea and G. Platero, Phys. Rev. Lett. **94**, 016806 (2005); Phys. Rev. B **76**, 073311 (2007).
- ²⁹A. D. Chepelianskii, A. S. Pikovsky, and D. L. Shepelyansky, Eur. Phys. J. B **60**, 225 (2007).
- ³⁰I. G. Finkler and B. I. Halperin, Phys. Rev. B **79**, 085315 (2009).
- ³¹I. A. Dmitriev, M. Khodas, A. D. Mirlin, D. G. Polyakov, and M. G. Vavilov, Phys. Rev. B **80**, 165327 (2009).
- ³²A. D. Chepelianskii, and D. L. Shepelyansky, Phys. Rev. B **80**, 241308 (2009).

- ³³D. Hagenmüller, S. De Liberato, and C. Ciuti, Phys. Rev. B **81**, 235303 (2010).
- ³⁴J. Inarrea and G. Platero, Nanotechnology **21**, 315401 (2010).
- ³⁵J. Iñarrea, R. G. Mani, and W. Wegscheider, Phys. Rev. B **82**, 205321 (2010).
- ³⁶S. A. Mikhailov, Phys. Rev. B **83**, 155303 (2011).
- ³⁷N. H. Lindner, G. Refael, and V. Galitski, Nat. Phys. **7**, 490 (2011).
- ³⁸Z. Gu, H. A. Fertig, D. P. Arovas, and A. Auerbach, Phys. Rev. Lett. **107**, 216601 (2011).
- ³⁹X. L. Lei and S. Y. Liu, Phys. Rev. B **84**, 035321 (2011); Phys. Rev. B **86**, 205303 (2012).

I. FIGURE CAPTIONS

Figure 1: (Color online) Top: A schematic of the measurement configuration showing the GaAs/AlGaAs Hall bar and the remote sensing resistor, R_s , located at the bottom of a cylindrical waveguide, within a low temperature cryostat. The panels (a) and (b) show the diagonal resistance (R_{xx}), Hall resistance (R_{xy}) and the fractional change of the remote detector resistance ($\Delta R_s/R_s(0)$) as functions of magnetic field, B , for sample S1. (a) R_{xx} (left panel) and R_{xy} (right panel) of S1 with (red curve) and without (black curve) 48 GHz microwave illumination. (b) Concurrent measurement of $\Delta R_s/R_s(0)$ with (red curve) and without (black curve) 48 GHz microwave excitation. The insets of (a) and (b) show the photoexcited R_{xx} and $\Delta R_s/R_s(0)$ signals over a broader B -range.

Figure 2: (Color online) (a) The dark- and photoexcited- at 48 GHz R_{xx} signal, and (b) the concurrently measured normalized remotely sensed signal $R_s/R_s(-0.2 \text{ T})$ for a high mobility GaAs/AlGaAs specimen. Various colored traces correspond to the different power levels over the range $0 \leq p \leq 3.2 \text{ mW}$. The blue upward arrows in (a) point out the inflections on the oscillatory resistance.

Figure 3: (Color online) The diagonal voltage V_{xx} and the remote sensor resistance R_s are exhibited for a GaAs/AlGaAs specimen S1 under 35 GHz microwave excitation. The different color curves correspond to discrete applied currents, I , through sample with $0 \leq I \leq 2.5 \mu\text{A}$. The same color code has been used in the top and bottom panels.

Figure 4: (Color online) The diagonal voltage V_{xx} and the remotely sensed signal R_s for a GaAs/AlGaAs 2DES subjected to 48 GHz microwave excitation. In plots (a) and (b), the applied current $I = 1 \mu\text{A}$. Plots (c) and (d) correspond to $I = 0 \mu\text{A}$. Note that the R_s signal remains unchanged upon switching off the current through the specimen.

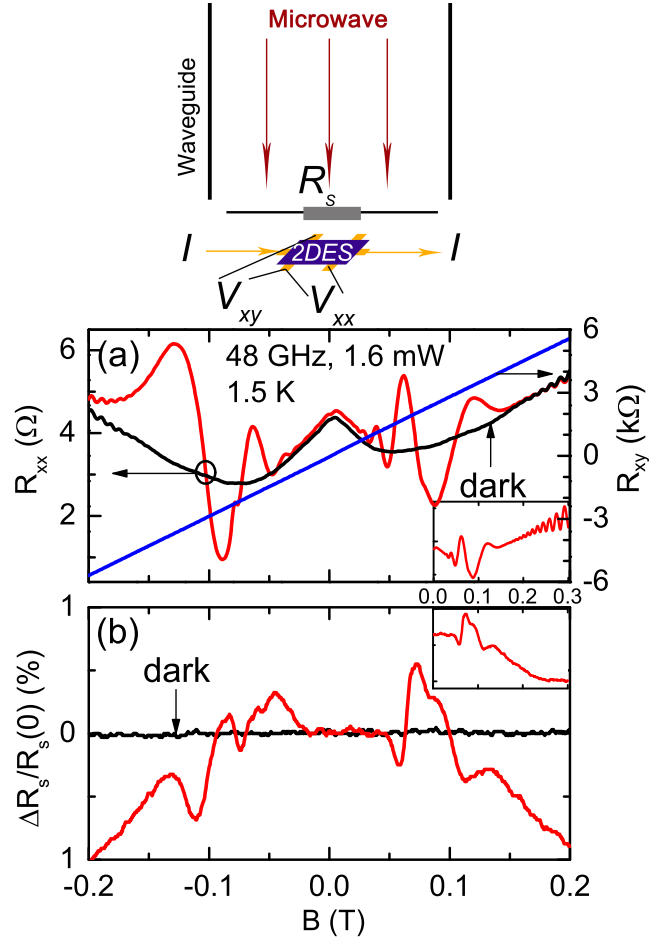


Figure 1

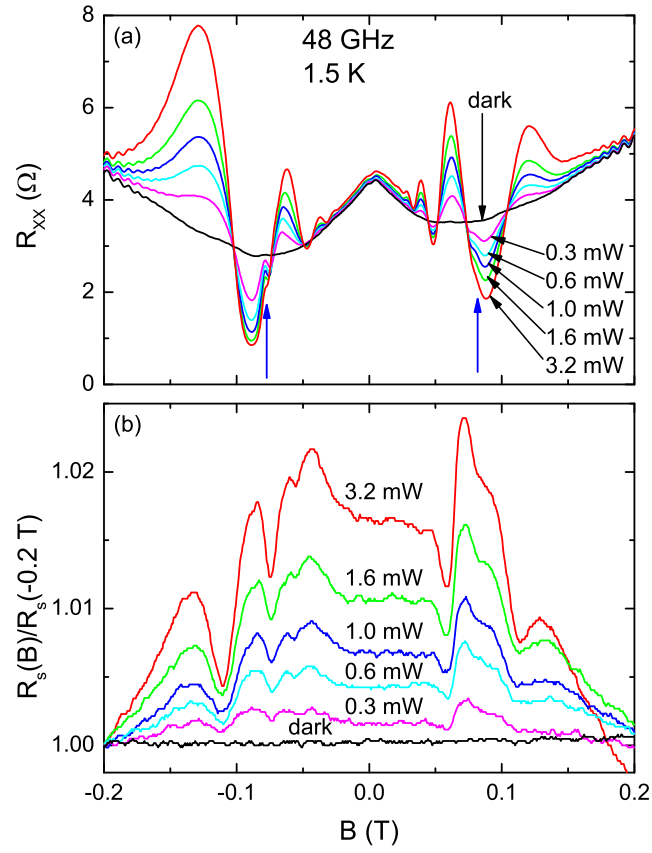


Figure 2

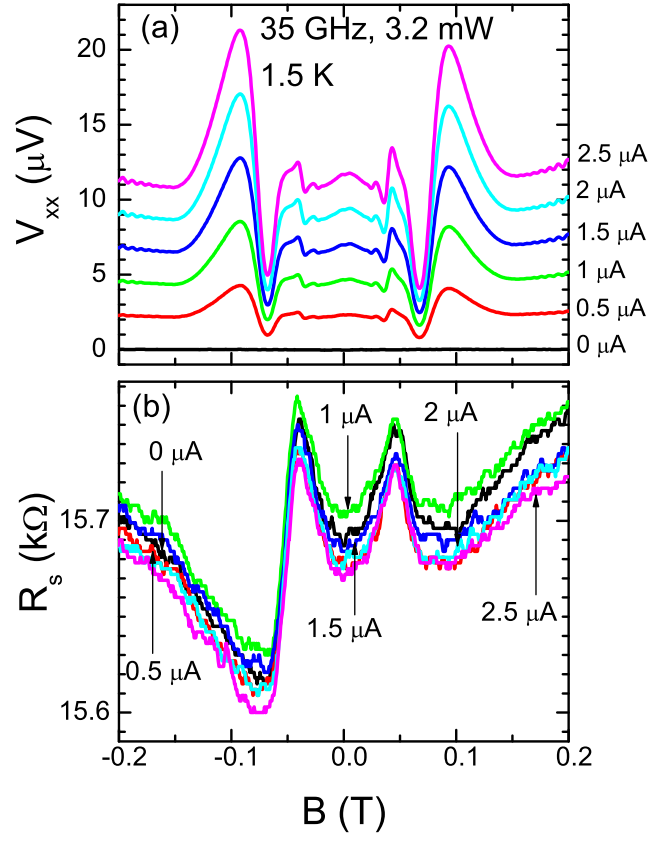


Figure 3

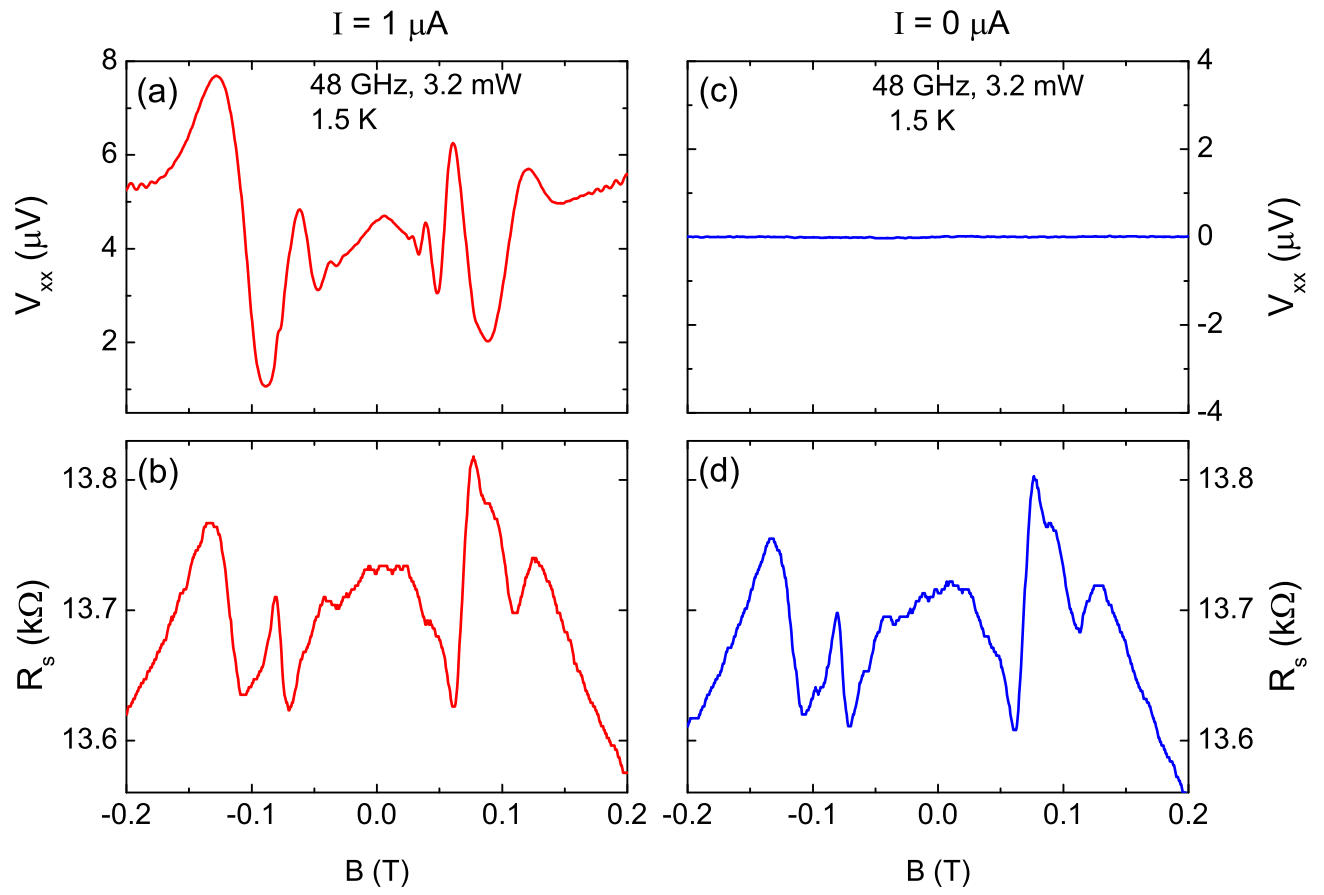


Figure 4